JOURNAL OF NANO- AND ELECTRONIC PHYSICS
Vol. **6** No 4, 04039(5pp) (2014)

ЖУРНАЛ НАНО- ТА ЕЛЕКТРОННОЇ ФІЗИКИ
Том **6** № 4, 04039(5cc) (2014)

Structural and Substructural Features of Apatite-biopolymer Composites: the Comparison of Data Obtained Using X-Ray Diffraction and Scanning Electron Microscopy with Electron Diffraction

V.M. Kuznetsov *, L.B. Sukhodub, L.F. Sukhodub†

Sumy State University, 2, Rimsky Korsakov Str., 40007 Sumy, Ukraine

(Received 08 April 2014; published online 29 November 2014)

In most cases, it is impossible to study and describe the structure and properties of samples using a single method. That is why in our studies two research methods were used and compared – X-Ray diffraction (XRD) and transmission electron microscopy (TEM) with electron diffraction (ED). Each method has certain advantages. In the case of the XRD – usability and more complex evaluation of the sample structural parameters. The advantages of the second one are the direct estimation of nanoparticle sizes and insignificant amount of the sample needed for the analysis. The main direction of our work is the studies and the analysis of the structural and substructural parameters of composite biomaterials based on apatite and presented in the shape of fine-dispersed powders, pastes and gels. Certain dependences of the sample structure and substructure on the initial agents and synthesis conditions were determined.

Keywords: X-Ray diffraction, Electron diffraction, Scanning electron microscopy, Hydroxyapatite, TEM, Biocomposites, Biomaterials.

PACS numbers: 87.85.J –, 87.64.Bx, 87.64.Ee

1. INTRODUCTION

In the majority of the cases it is impossible to describe and study the structure and properties of the samples using only one method. Therefore, two investigation methods, namely, X-ray diffraction (XRD) and transmission electron microscopy (TEM) with electron diffraction (ED) are used in the present work.

The XRD method allows to determine the phase composition of the samples, evaluate the crystallite sizes in different crystallographic planes, microstrain values, unit cell parameters, etc.

TEM allows to directly measure the sizes of particles (of groups of crystals, separate crystals or crystallites) of the sample, ED allows to determine the phase composition of the samples and unit cell parameters.

Convenience and a more complete evaluation of the structural parameters of the samples are the advantages of the first method; advantages of the second one consist in the directness of the obtained results and insignificant amount of the sample necessary for the analysis. However, when determining the sizes of nanoparticles, both methods have their own disadvantages. The first method determines the coherent-scattering region (CSR) size, which although is usually identified with the average crystallite size, actually differs from it. Both the measurement errors of the nanoparticle sizes and subjectivity of the choice of concrete nanoparticles for the calculation are the drawbacks in the case of the second method.

It is generally known that the physical properties of a bone depend on its structural organization. The main structural components of the native bone tissue are the organic constituent represented by collagen of the type I and the inorganic one represented by hydroxyapatite (HA). Here, inorganic constituent provides bones with strength, and organic one – with elasticity. Presence of nanosize apatite crystals which are the inorganic environment of collagen fibrils is a unique factor ascribed to the bone strength. Biologic apatites are nonstoichiometric (atomic ratio Ca/P < 1.67), calcium-deficient (cation substitutions by sodium ions take place most often), contain a substantial amount of carbonate ions [1]. Among the requirements in the development of novel biomaterials based on calcium phosphates are the following: maximum similarity of artificial materials in properties and structure with the natural ones, acceleration of the integration process into the organism tissues, absence of immune reactions, osteostimulative action and possibility of their gradual substitution by new bone tissue.

The aim of the present work is the complementary use and comparison for the investigation of two methods, such as TEM with ED and XRD. The main focus area is the study and analysis of the structural and substructural parameters of composite biomaterials based on apatite represented in the form of fine powders, pastes and gels for further enhancement of the synthesis mechanisms of biocomposites and improvement of the techniques of their study.

2. MATERIALS AND METHODS

2.1 Synthesis

2.1.1 Fine powders

Sample No1. Calcium acetate $Ca(CH_3COO)_2$ (0.3 M), sodium dihydrogen phosphate NaH_2PO_4 (0.2 M), sodium hydrocarbonate $NaHCO_3$ (0.01 M), 18 mas. % of NaOH solution were the initial substances for the synthesis by the "wet chemistry" method of calcium-deficient HA with the content of carbonate ions. Synthesis was performed at room temperature and pH = 10.3, and then the sample was centrifuged, dried at 37 °C and annealed at 900 °C for further study. Formation of calcium-deficient HA was carried out according to the following reaction:

* vkuznetsov.ua@gmail.com
† l_sukhodub@yahoo.com

$$(10-x)\mathrm{Ca(CH_3COO)_2}+(6-x)\mathrm{NaH_2PO_4}+ \\ +x\mathrm{NaHCO_3}++14\mathrm{NaOH}= \\ =\mathrm{Ca_{10-x}Na_x(PO_4)_{6-x}(CO_3)_x(OH)_2}+ \\ +(20-x)\mathrm{CH_3COONa}+12\ \mathrm{H_2O}. \quad (1)$$

Sample No2. Production of the powder of calcium-deficient HA was performed by the synthesis procedure of the Sample 1 according to the reaction (1). Moreover, aqueous solution (4 g/l) of sodium salt of carboxymethyl cellulose (CMC) was added to the working mixture for the purpose of the formation of HA in the form of nano-particles. Na-CMC solution has an increased viscosity, and in our experiment it was used as the surface-active substance for the prevention of agglomeration of the formed calcium-phosphate particles. Content of CMC in the finished product accounts for about 10 %. Mixture of agents was mixed in a shaker at the temperature of 70 °C with the velocity of 254 revolutions per minute during 2 hours. After 24 hour aging at room temperature, the product was thoroughly washed to pH = 7.4, centrifuged, dried at 37 °C and annealed at 900 °C for further investigations.

2.1.2 Pastes

Sample No3. For the formation of biomaterial in the form of a paste, a stoichiometric HA (Ca/P = 1.67) was obtained from the solution consisted of calcium nitrate $Ca(NO_3)_2 \times 4H_2O$ and ammonium hydrophosphate $(NH_4)_2HPO_4$. HA formation was carried out according to the following reaction:

$$10\mathrm{Ca(NO_3)_2}\times 4\mathrm{H_2O}+6\mathrm{(NH_4)_2HPO_4}+ \\ +8\mathrm{NH_4OH}=\mathrm{Ca_{10}(PO_4)_6(OH)_2}+ \\ +20\mathrm{NH_4NO_3}+46\mathrm{H_2O}. \quad (2)$$

The synthesis was performed at the temperature of 80 °C and pH = 12. The obtained product after its aging during 24 hours was repeatedly washed by deionized water to pH = 7.4. After this, solid and liquid fractions were separated by centrifugation (5000 rev/min, 10 min). Then, the sample was dried at 37 °C and annealed at 900 °C for further investigations. A part of the solid fraction with the humidity of 14 %, was dried at the temperature of 37 °C. Material of the humid and dried solid fractions was used for the preparation of a dense paste (final humidity is 43 %) of the following composition: solid fraction (in terms of HA dry powder) – 57 %, liquid fraction (deionized water) – 43 %.

2.1.2 Hydrogels

Recently, the use of materials in the form of hydrogels gains more popularity. Structure of polymer chains, which form a three-dimensional gel network, gives the possibility to immobilize and hold a sufficient amount of water, biological liquid or medicine [2, 3].

In the present work, we have studied the composite materials consisting of

a) polymer matrix and inorganic filler which in full measure model the bone tissue (samples No4 and No5). Chitosan was used as the polymer matrix in the sample No4 and sodium alginate – in the sample No5. During the synthesis of these samples HA was formed according to the following reaction:

$$10\mathrm{CaCl_2}+6\mathrm{H_3PO_4}+20\mathrm{NaOH}\rightarrow \\ \mathrm{Ca_{10}(PO_4)_6(OH)_2}+20\mathrm{NaCl}+18\mathrm{H_2O}; \quad (3)$$

b) calcium-phosphate compounds, whose particles are immobilized in the three-dimensional matrix formed by hydrogen bonds (sample No6). HA synthesis for this sample occurred by reaction (2) with addition of silver ions or partial substitution of calcium atoms in the initial product.

Synthesis technique of the specified samples is represented below.

Sample No4. The starting substances for the preparation of the composite material were phosphoric acid H_3PO_4 (0.06 M), anhydrous calcium chloride $CaCl_2$ (0.1 M), aqueous solution of sodium hydroxide NaOH (10 M), chitosan with the molecular mass of 39 kDa. Synthesis was performed by the "wet chemistry" method at room temperature and pH = 7. After aging of the solution during 14 days, the sediment was thoroughly washed by deionized water with separation of the solid fraction by centrifugation, and then sterilized. Then, the sample was dried at 37 °C and annealed at 900 °C for further investigations. The degree of humidity of the obtained gel was equal from70 до 88 %. Composition of the solid fraction: HA from 60 to 90 %, chitosan – from 10 to 40 %.

Sample No5. The starting substances for the preparation of the composite material were phosphoric acid H_3PO_4 (0.06 M), anhydrous calcium chloride $CaCl_2$ (0.1 M), aqueous solution of sodium hydroxide NaOH (10 M), aqueous 1 mas. % solution of sodium alginate. Synthesis of the composite material was carried out by the "wet chemistry" method at room temperature and pH = 10.6. After mixing of reagents, the mixture was treated by ultrasound during 10 minutes. After aging of the solution during 10 days, the sediment was thoroughly washed by deionized water with separation of the solid fraction by centrifugation and sterilized. Then, the sample was dried at 37 °C and annealed at 900 °C for further investigations. The degree of humidity of the obtained gel was equal from 70 до 88 %. Composition of the solid fraction: HA 82 %, alginate – 18 %.

Sample No6. A hydrogel containing silver ions was obtained from the solution composed of 0.167 M calcium nitrate $Ca(NO_3)_2 \times 4H_2O$ and 0.1 M ammonium hydrophosphate $(NH_4)_2HPO_4$. Silver nitrate at 10 mas. % of the amount of calcium ions was added to the solution. Synthesis took place at the temperature of 80 °C and pH = 12. The obtained product after its aging during 24 hours and repeated washing by deionized water to pH = 7.4 was centrifuged, dried at 37 °C and annealed at 900 °C for further study.

2.2 TEM with ED

Electron-microscopic investigations of the structure and phase composition of the samples were carried out using the transmission electron microscope PEM-125K when operating in the bright-field and microdiffraction mode without the introduced selective diaphragm. The accelerating voltage was equal to 90 kV.

When operating in the microdiffraction mode, the diffraction pattern was obtained from the chosen, insignificant in size sample region, whose area is less than at usual diffraction. This method allows to obtain results from a small sample area that is important in the study of the microstructure and multiphase samples.

Support copper (30 × 30 μm) and nickel (50 × 50 μm) nets were used for the arrangement of objects in the object plane of the PEM objective lens. Since the objects sizes were less than the net holes, they were placed on thin, transparent for electrons, continuous carbon films of the thickness of 20 nm. The given samples were deposited on the support net with the carbon film prefastened in a grid due to dispergation of suspension by ultrasonic method. The suspension was obtained by the gel (powder) solution method by distillate water.

2.3 X-ray diffraction

The X-ray diffraction study of the samples structure was performed on the automated diffractometer DRON-3 (LTD "Burevestnik", www.bourevestnik.ru). Automation system DRON-3 is based on the microprocessor controller which provides the control of the goniometer GUR-8 and data transmission in the digital form to PC.

CuKα-radiation (wavelength 0.154 nm), θ-2θ Bragg-Brentano focusing (2θ is the Bragg angle) were used in the survey. The values of the current strength and voltage on the X-ray tube were equal to 20 mA and 40 kV, respectively. A survey of the samples was carried out in the continuous registration mode (rate 1°/min), range of angles 2θ from 10° to 90°.

For the Bragg-Brentano focusing, the X-ray tube focus and receiving slot of the detector are located on the goniometer circle, in the center of which a plane sample is placed. Detection of the diffraction spectrum is performed for a synchronous rotation of the detector and the sample around the goniometer axis; and the angular rate of the detector rotation is two times larger than that for the sample. Quanta of the X-ray radiation diffracted from the sample are transformed by the detection block into electric pulses which after leaving the detection block undergo amplification, amplitude discrimination, and later are used as the information signal for measurement and detection of the pulse counting rate of the X-ray radiation.

Experimental results were transmitted directly to the experimental support package DifWin-1 (LTD "Etalon-Ts", www.specord.ru) for the preprocessing. Identification of the crystal phases was performed using the JCPDS file (Joint Committee on Powder Diffraction Standards).

3. RESULTS AND DISCUSSION

The phase analysis performed by the ED and XRD methods has shown that only one phase – HA (JCPDS 9-432, Ca/P = 1.67, hexagonal system) – is present in all the samples. For the study of the initial apatite structure, the temperature testing of the samples by their annealing at 900 °C during 1 hour was performed, since at this temperature both the recrystallization and phase decomposition processes take place that can lead to the formation of other calcium-phosphate phases, for example, tricalcium phosphate (TCP).

The nanoparticles sizes in length D were measured using the TEM images, since they have a filamentary structure in all the cases. By the ED we have obtained the interplanar distances d_{hkl} (h, k are l the Miller indices) of the samples, established their phase composition and calculated the unit cell parameters a and c (for JCPDS 9-432 $a = 0.942$ nm, $c = 0.688$ nm) by the diffraction lines which correspond to the crystallographic planes (3 1 0) and (0 0 2) by the following formulas:

$$a_{hk0} = 2d_{hk0}\frac{\sqrt{3}}{3}\sqrt{h^2 + hk + k^2} \text{ i } c_{00l} = l \cdot d_{00l}, \qquad (4)$$

where a_{hk0} is the unit cell parameter calculated in the plane (h k 0); d_{hk0} is the interplanar distance of the plane (h k 0), h, k and l are the Miler indices; c_{00l} is the unit cell parameter calculated in the plane (0 0 l); d_{00l} is the interplanar distance of the plane (0 0 l).

By the XRD data, we have established the phase composition of the samples and calculated the crystallite sizes and microstrain level using the method described below along the [0 0 c] crystallographic direction.

The average crystallite size by Scherrer is calculated by the following formula [4]:

$$L = \frac{K\lambda}{\beta_m \cos\theta}, \qquad (5)$$

where K is the dimensionless constant dependent on the crystallite shape (we take $K = 1$); λ is the X-ray radiation wavelength; β_m is the integral width of the diffraction profile, physical extension in which occurs only due to small sizes of the CSR; θ is the diffraction angle.

Microstrain level ε is measured as the change in the interplanar distance of the studied sample compared with the standard, in which microstrains are absent. If physical extension of diffraction lines occurs only through the crystal lattice microstrain, then the microstrain level is determined by the following formula:

$$\varepsilon = \frac{\beta_n}{4\mathrm{tg}\theta}, \qquad (6)$$

where β_n is the integral width of the diffraction profile, in which physical extension occurs only through the crystal lattice microstrain.

An experimental extension of diffraction lines B consists of the physical β and instrumental b ones. Since in our case diffraction lines are approximated most precisely by the Cauchy function, then $B = \beta + b$. If both the small size of the CSR and presence of the crystal lattice microstrains influence the value of the physical extension, then $\beta = \beta_m + \beta_n$. Hence, taking into account (5) and (6), we will obtain

$$\beta = \frac{\lambda}{L\cos\theta} + 4\varepsilon\mathrm{tg}\theta. \qquad (7)$$

The TEM images and electron diffraction patterns are shown in Fig. 1. The X-ray diffraction patterns are represented in Fig. 2-Fig. 4. The structural and substructural parameters of the samples obtained using both methods are given in Table 1.

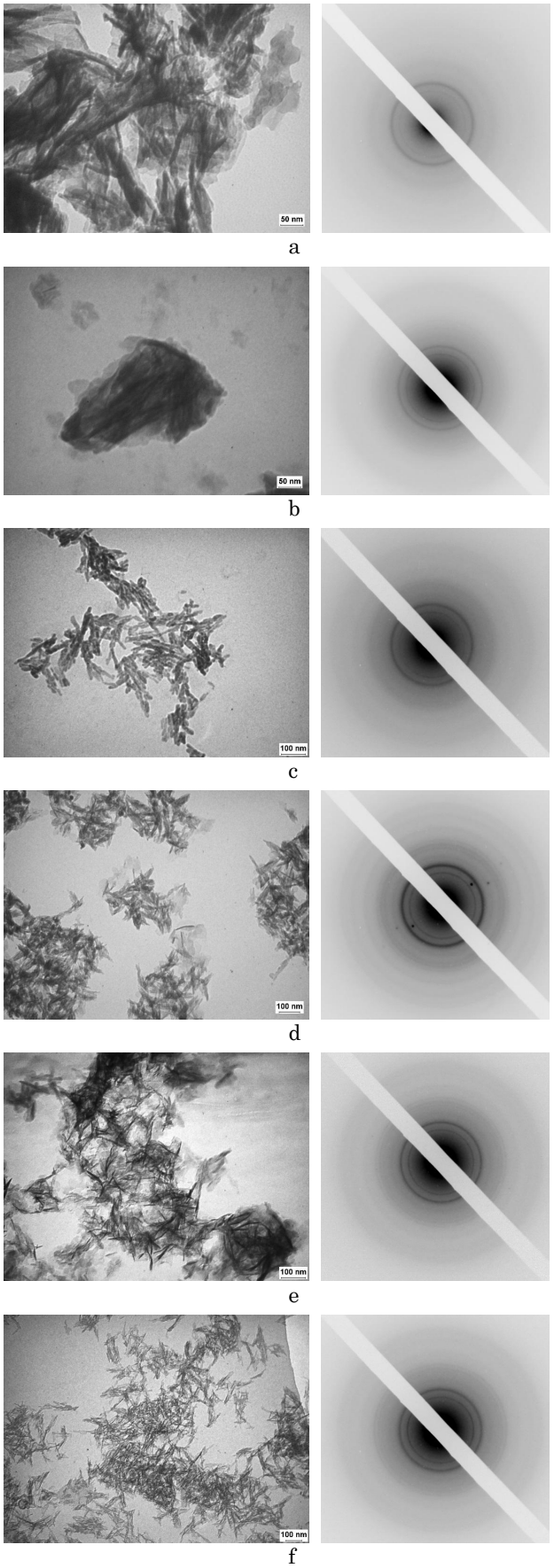

Fig. 1 – TEM images and ED pictures of the samples No1 (a), No2 (b), No3 (c), No4 (d), No5 (e), No6 (f)

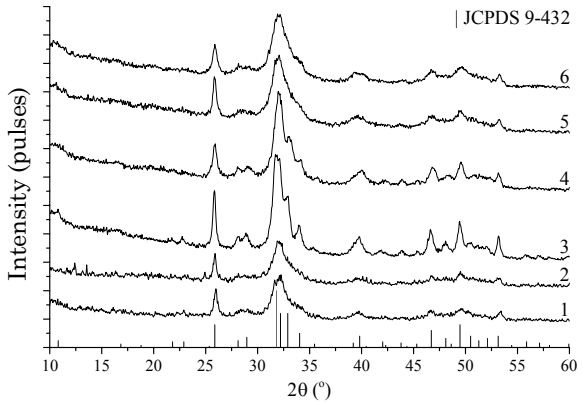

Fig. 2 – Diffraction patterns of the initial samples dried at 37 °C

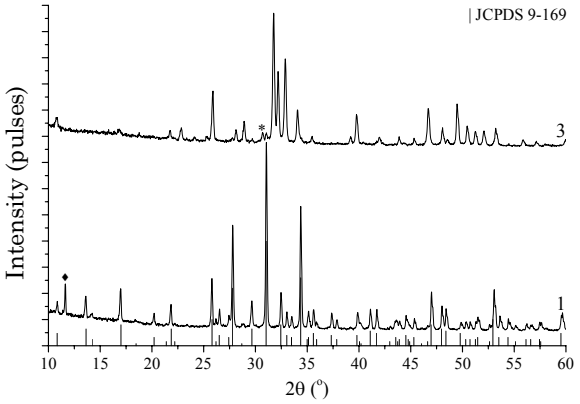

Fig. 3 – Diffraction patterns of the samples No1 and No3 after annealing (symbols ♦ and * denote the main peaks of brushite and α-TCP, respectively)

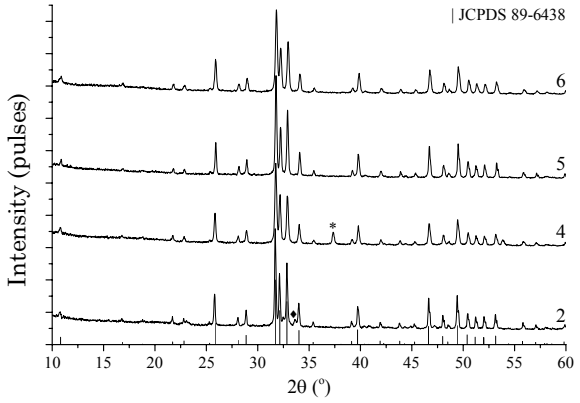

Fig. 4 – Diffraction patterns of the samples No2, 4, 5, 6 after annealing (symbols ♦ and * denote the main peaks of $NaCaPO_4$ and CaO, respectively)

Table 1 – Structural and substructural parameters of the samples by the TEM with ED and XRD data

Samples	Initial					After annealing	
	TEM and ED			XRD		XRD	
	a, nm	c, nm	D, nm	L, nm	$\varepsilon \cdot 10^3$	L, nm	$\varepsilon \cdot 10^3$
1	0.933	0.684	~ 120	33.2	1.092	49.4*	0.87*
2	0.941	0.690	~ 120	29.7	0.552	63.8	0.21
3	0.953	0.696	~ 80	23.2	1.197	50	0.031
4	0.949	0.688	~ 80	14.3	3.220	55.4	0.001
5	0.945	0.688	~ 80	24.6	0.228	58.6	0.3
6	0.912	0.676	~ 80	17.2	0.647	45.7	0.28

* are given along the crystallographic direction [a b 0]

Although the nanoparticle sizes obtained using TEM significantly (almost 4 times, see Table 1) differ from the crystallite sizes calculated with the XRD along the crystallographic direction [0 0 *c*], they are in a certain correlation that can indicate the orientation of crystallites in this direction.

X-ray phase (XRP) analysis of the sample No1 after annealing has shown the presence of two phases, such as β-TCP (JCPDS 9-169, at. Ca/P = 1.5) and brushite (JCPDS 11-293, at. Ca/P = 1) that implies the calcium deficiency of the initial apatite that conditions a slightly increased microstrain level.

Investigation of the sample No2 after annealing by the XRP implies the presence of two phases, such as HA (JCPDS 8-6438, at. Ca/P = 1.67, concentration is 95 %) and $NaCaPO_4$ (JCPDS 29-1193, at. Ca/P = 1, concentration is 5 %) that indicates a nonstoichiometry of the initial apatite probably because of the presence of a polymer inside, namely CMC. Concentrations of the phases were calculated by the method of alumina numbers [6].

In the sample No3 XRP analysis after annealing has shown the presence of three phases: HA (JCDPS 9-432, at. Ca/P = 1.67, concentration is 86 %), α-TCP (JCDPS 9-348, at. Ca/P = 1.5, concentration is 11 %) and β-TCP (JCDPS 9-169, at. Ca/P = 1.5, concentration is 3 %). In this case, atomic ratio Ca/P calculated by the technique given in [5] is equal to 1.64. An increased microstrain level can be explained by a large amount of the liquid fraction in the initial form.

Based on the XRP analysis, sample No4 consists of two phases, such as HA (JCDPS 9-432, at. Ca/P = 1.67, concentration is 97 %) and CaO (JCDPS 37-1497, concentration is 3 %). The presence of another phase after thermal test indicates a nonstoichiometry of the initial apatite. The main factor, which conditions a small size of crystallites and high microstrain level, is certainly the addition of chitosan that, as the previous investigations [7] have shown, worsens the apatite crystallinity.

In the samples No5 and No6 the XRP analysis after annealing has shown the presence of only one phase – HA (JCPDS 9-432, at. Ca/P = 1.67) that indicates a stoichiometry of the initial apatite.

4. CONCLUSIONS

Application of two methods, namely, TEM with ED and XRD, for the investigation of the samples has clear advantages over the use of only one of them. This approach allows to determine the unit cell parameters even for the initial apatite, for which in the majority of the cases because of a low crystallinity and, correspondingly, a low resolution of diffraction lines it is impossible to perform this and also to obtain both the crystallite sizes and sizes of the directly formed nanoparticles.

Nanoparticles sizes obtained using TEM considerably (almost 4 times) differ from the crystallite sizes calculated by the XRD along the crystallographic direction [0 0 *c*]. This indicates that nanoparticles consist of not separate crystallites but also their groups.

It is shown that addition of chitosan to a composite material leads to the deterioration of the crystal structure of the initial apatite. In the given case, this is implied by a small size of the crystallites and a large value of the microstrain level in comparison with other samples. Also, a high microstrain level is observed in the material with a significant amount of liquid fraction in the initial form. A more detailed analysis of the apatite-chitosan (alginate) composites using, including, the IR-spectroscopy with the Fourier analysis, is represented in our recent review [8].

REFERENCES

1. S.M. Barinov, *Biokeramika na osnove fosfatov kal'tsiya* (M.: Nauka: 2005).
2. J.L. Drury, D.J. Mooney, *Biomaterials* **24**, 4337 (2003).
3. B.K. Mann, *Clin. Plast. Surg.* **30**, 601 (2003).
4. H.P. Klug, L.E. Alexander, *X-Ray Diffraction Procedures: For Polycrystalline and Amorphous Materials* (New York: Wiley: 1974).
5. S. Raynaud, E. Champion, D. Bernache-Assollant, J.-P. Laval, *J. Am. Ceram. Soc.* **84**, 359 (2001).
6. F.H. Chung, *J. Appl. Crystallogr.* **8**, 17 (1975).
7. S.N. Danilchenko, O. V. Kalinkevich, V.N. Kuznetsov, A.N. Kalinkevich, T.G. Kalinichenko, I.N. Poddubny, V.V. Starikov, A.M. Sklyar, L.F. Sukhodub, *Cryst. Res. Technol.* **45**, 685 (2010).
8. L.F. Sukhodub, G.O. Yanovska, L.B. Sukhodub, V.M. Kuznetsov, O.S. Stanislavov, *J. Nano- Electron. Phys.* **6** No1, 01001 (2014).